

# Spindle assembly checkpoint signaling and sister chromatid cohesion are disrupted by HPV E6-mediated transformation

Hazheen K. Shirnekhi, Erin P. Kelley, Jennifer G. DeLuca\*, and Jacob A. Herman<sup>†,\*</sup>

Department of Biochemistry and Molecular Biology, Colorado State University, Fort Collins, CO 80523

**ABSTRACT** Aneuploidy, a condition that results from unequal partitioning of chromosomes during mitosis, is a hallmark of many cancers, including those caused by human papillomaviruses (HPVs). E6 and E7 are the primary transforming proteins in HPV that drive tumor progression. In this study, we stably expressed E6 and E7 in noncancerous RPE1 cells and analyzed the specific mitotic defects that contribute to aneuploidy in each cell line. We find that E6 expression results in multiple chromosomes associated with one or both spindle poles, causing a significant mitotic delay. In most cells, the misaligned chromosomes eventually migrated to the spindle equator, leading to mitotic exit. In some cells, however, mitotic exit occurred in the presence of pole-associated chromosomes. We determined that this premature mitotic exit is due to defects in spindle assembly checkpoint (SAC) signaling, such that cells are unable to maintain a prolonged mitotic arrest in the presence of unaligned chromosomes. This SAC defect is caused in part by a loss of kinetochore-associated Mad2 in E6-expressing cells. Our results demonstrate that E6-expressing cells exhibit previously unappreciated mitotic defects that likely contribute to HPV-mediated cancer progression.

## Monitoring Editor

Kerry S. Bloom  
University of North Carolina

Received: Dec 15, 2016

Revised: May 18, 2017

Accepted: May 18, 2017

## INTRODUCTION

A majority of cancer cells exhibit defects in chromosome segregation, which in many cases result in aneuploidy, a situation by which cells contain either too few or too many whole chromosomes (Gordon *et al.*, 2012). Although defects in regulating kinetochore–microtubule attachments are a well-demonstrated cause of chromosome segregation errors, it is unclear how oncogenic proteins induce such defects (Cimini *et al.*, 2001; Bakhoun *et al.*, 2009a). Expression of E6 and E7 proteins isolated from high-risk human papillomavirus (HPV) strains 16 and 18 are sufficient to induce aneuploidy and other behaviors common to cancer cells (Duensing and Münger, 2002). Thus expression of these single proteins makes for a useful genetic model of

possible mitotic defects that lead to chromosome segregation errors.

HPV E6 transforming protein is best known for functioning in complex with E6AP/UBE3A to polyubiquitinate p53 and target it for proteasomal degradation (Scheffner *et al.*, 1993). By degrading p53, HPV-positive cells are able to bypass the senescence program usually activated by aneuploidy/polyploidy; however, p53 loss is not sufficient to cause chromosome segregation defects (Thompson *et al.*, 1997). HPV E7 transforming protein is instead best known for its sequestration of pRb, which accelerates the cell cycle. Upon inhibition of pRb by E7, the transcription factor E2F is constitutively active, deregulating the G1- to S-phase transition (Liu *et al.*, 2006). Thus HPV-positive cells exhibit unregulated cell cycling; however, unrestrained cell growth alone does not cause chromosome segregation defects either. Thus the molecular mechanisms by which E6 and E7 induce mitotic defects and chromosome segregation errors remain largely unexplained.

The correct segregation of chromosomes is a complex task accomplished by the entire mitotic machinery. Two major mitotic regulatory mechanisms are the spindle assembly checkpoint (SAC) and kinetochore–microtubule attachment error correction. The SAC ensures genetic fidelity by preventing mitotic exit until all kinetochores are properly attached to microtubules of the mitotic spindle and each sister kinetochore pair achieves biorientation at the spindle

This article was published online ahead of print in MBoC in Press (<http://www.molbiolcell.org/cgi/doi/10.1091/mbc.E16-12-0853>) on May 24, 2017.

<sup>†</sup>Present address: Fred Hutchinson Cancer Research Center, Seattle, WA 98109.

\*Address correspondence to: Jacob Herman ([jherman@fredhutch.org](mailto:jherman@fredhutch.org)) or Jennifer DeLuca ([jdeluca@colostate.edu](mailto:jdeluca@colostate.edu)).

Abbreviations used: HPV, human papillomavirus; SAC, spindle assembly checkpoint.

© 2017 Shirnekhi *et al.* This article is distributed by The American Society for Cell Biology under license from the author(s). Two months after publication it is available to the public under an Attribution–Noncommercial–Share Alike 3.0 Unported Creative Commons License (<http://creativecommons.org/licenses/by-nc-sa/3.0>).

“ASCB®,” “The American Society for Cell Biology®,” and “Molecular Biology of the Cell®” are registered trademarks of The American Society for Cell Biology.

equator (Musacchio and Salmon, 2007; Lara-Gonzalez *et al.*, 2012). Error correction instead employs phosphoregulation of microtubule-binding proteins and microtubule depolymerases to ensure that only properly bioriented kinetochore–microtubule attachments are stabilized (Knowlton *et al.*, 2006; Bakhom *et al.*, 2009b; DeLuca *et al.*, 2011).

Here we investigate how the fidelity of chromosome segregation is affected by expression of HPV proteins E6 and E7. Specifically, we analyzed cells' ability to generate and regulate kinetochore–microtubule attachments and to generate a robust SAC response. Through this characterization, we demonstrate that HPV16 E6 induces chromosome segregation errors by preventing proper chromosome congression, weakening the SAC, and compromising sister chromatid cohesion. These studies clarify how E6 contributes to chromosome segregation defects and aneuploidy and may help elucidate how such errors arise in other cancers.

## RESULTS AND DISCUSSION

### Expression of HPV16 E6 and E7 transforms RPE1 cells

We performed these studies in an hTert immortalized epithelial cell line, RPE1, a common tool to investigate mitotic processes in a non-transformed background. E6 and/or E7 genes from high-risk strain HPV16 were stably introduced into RPE1 cells using Moloney murine leukemia virus (MMLV)-based retroviral transduction (Halbert *et al.*, 1991). Gene expression was driven from a combination of the MMLV LTR and the HPV16 E6 endogenous p97 promoter (Figure 1A). Cells were termed RPE1, RPE16, RPE17, and RPE167 to denote which transgene each expressed. Polyclonal populations were negatively selected via neomycin resistance, and transgene expression was validated by PCR analysis of cDNA after 3 wk of selection/outgrowth (Figure 1B). Expression of HPV proteins E6 and/or E7 was sufficient to cause changes in cell morphology; all cells were less elongated and

contained dark staining nuclei, similar to transformed cells (Figure 1C). In addition to phenotypic changes, expression of E6 and/or E7 also conferred anchorage-independent growth to RPE1 cells. Most cells isolated from tumors can proliferate in a three-dimensional matrix and give rise to spherical colonies. This behavior is correlated with transformation, metastatic potential, and tumor-initiating ability (Shin *et al.*, 1975; Halbert *et al.*, 1991; Mori *et al.*, 2009). Nontransformed RPE1 cells were not able to proliferate in soft agar, and expression of either HPV protein conferred this behavior (Figure 1D). On average, RPE16 cells demonstrated limited growth (3 colonies/field), whereas RPE17 cells grew more robustly (10 colonies/field), and combined expression was synergistic (21 colonies/field). E6 and E7 inactivate tumor suppressor genes to bypass cell cycle checkpoints, particularly the G1/S transition, which contributes to their tumorigenic activities (Scheffner *et al.*, 1993; Liu *et al.*, 2006). In RPE1 cells expressing either E6 or E7, we observed a significant decrease in population doubling time (Figure 1E), which is in agreement with a shortened G1 due to loss of p53 and pRb activity (Figure 1E). Consistent with these oncogenic properties and with previous reports (Duensing and Münger, 2002), expression of E6 and/or E7 also induced significant aneuploidy, with the modal chromosome number increasing by 10–20 chromosomes (Figure 1F). In contrast to previous reports, we rarely observed polyploid cells (Thomas and Laimins, 1998) and instead found a small population of hypodiploid cells.

### E6 and E7 induce aneuploidy through unique chromosome segregation errors

In all transduced lines, aneuploid cells were commonly observed, whereas polyploid cells were not, suggesting that in this system, HPV proteins were acting on mitotic processes (e.g., spindle formation, SAC activity, kinetochore–microtubule attachments) rather than the cytokinesis machinery to induce chromosome segregation

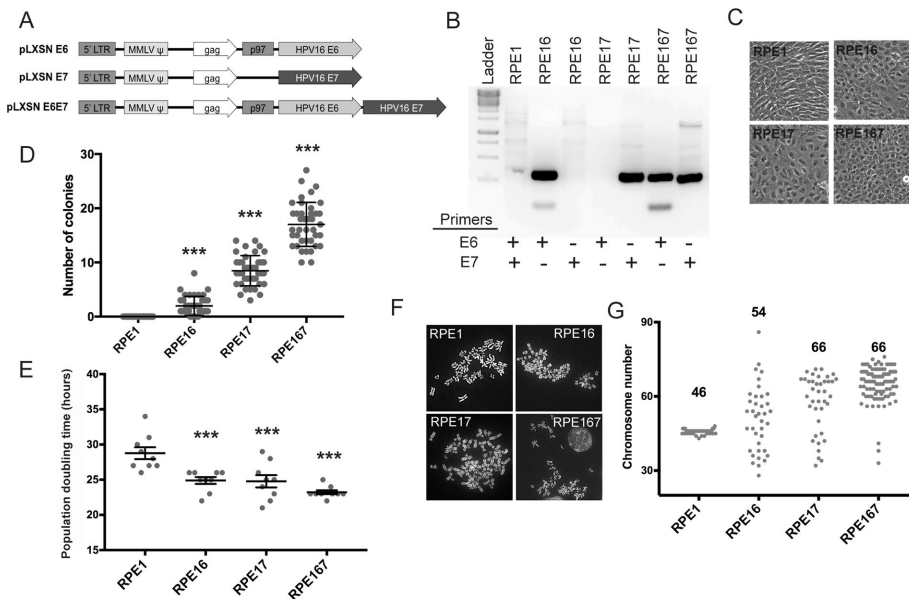


**FIGURE 1:** Expression and characterization of HPV16 E6 and E7 in RPE1 cells. (A) Schematic of pLXSN expression cassettes used to produce HPV 16 E6 and E7 proteins in RPE1 cells. (B) Reverse transcription PCR validation of gene expression in virally transduced cells. (C) HPV proteins induce changes in cell morphology. (D, E) Expression of E6 and/or E7 increases cells' ability to grow independent of anchorage in soft agar (D) and decreases population doubling time (E). (F, G) Chromosome spreads demonstrating the ability of E6 and E7 to induce aneuploidy in RPE1 cells; polyploidy is rarely observed. (G) Chromosome numbers for each cell line and the population mode for each. Mean values are reported unless stated otherwise; error bars are SD of data collected from three experiments. Two-sided Student's *t* test, \*\*\**p* < 0.001.

defects. To directly test this, we imaged E6/E7-transduced cells additionally expressing histone H2B–green fluorescent protein (GFP) progressing through mitosis and documented the various types of mitotic errors. E7 expression resulted in a small but significant increase in the instance of lagging chromosomes (~3%; Figure 2, A and B). Lagging chromosomes are common in cancer cells and usually arise from merotelic attachments, where a single kinetochore is bound to microtubules from both spindle poles (Cimini *et al.*, 2001; Bakhom *et al.*, 2009a). The mechanisms leading to merotelic attachments are well established, and thus we focused on E6 expression, which resulted in a more novel phenotype in which ~22% of cells had a small number (one to four) of chromosomes remaining at one or both of the spindle poles in a cell whose chromosomes were otherwise bioriented (Figure 2, A and B). This finding was further validated in an hTert immortalized lung fibroblast line (Supplemental Figure 1, A–C). Both E6- and E7-expressing cells took longer to progress through mitosis (nuclear envelope breakdown to anaphase onset) than control RPE1 cells (Figure 2C). HPV proteins increased the median mitotic duration by 25–35%, and this increase observed in E6-expressing cells

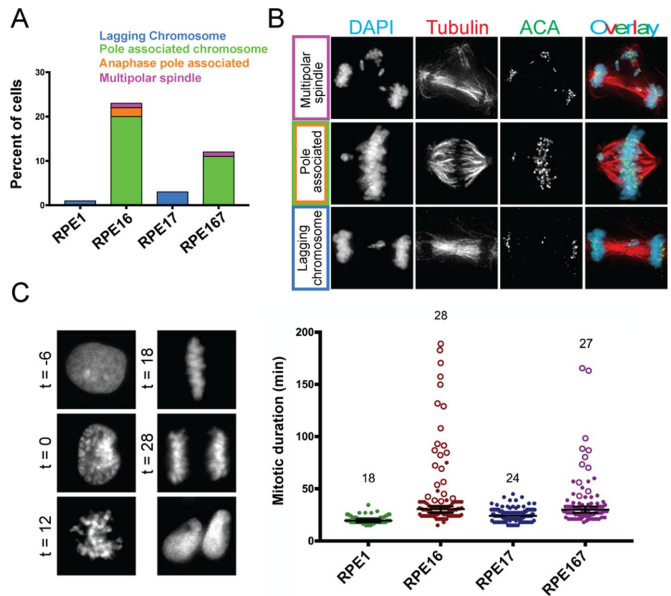


**FIGURE 2:** HPV proteins induce mitotic errors and delay mitotic duration. (A) Chromosome alignment/segregation errors identified by live-cell filming of RPE cells expressing histone H2B-GFP to identify chromatin. At least 150 cells/line were quantified. (B) High-resolution immunofluorescence staining of RPE16 and RPE17 cells demonstrating errors quantified in A. (C) Left, representative images of a histone H2B-GFP-expressing RPE1 cell transiting mitosis (nuclear envelope breakdown to anaphase onset) with time shown in minutes. Right, median mitotic duration for each cell line. Open circles denote cells with pole-associated chromosomes. Error bars are 95% confidence interval of median values.

was largely due to a small population that required 50–200 min to complete mitosis. This population was composed of RPE16 cells with pole-associated chromosomes that remained in mitosis for 80 min on average until the chromosome(s) migrated to the spindle equator and anaphase began (Figure 2C, open circles). Whereas most cells were eventually able to align all chromosomes, a small percentage of cells (~2%) initiated anaphase before the pole-associated chromosomes (termed anaphase pole associated) could congress to the metaphase plate (Figure 2A). This suggested that E6-expressing cells initially stimulated a functional checkpoint but failed to arrest cells in mitosis for prolonged periods despite the presence of uncongressed chromosomes.

### E6 weakens SAC signaling by decreasing Mad2 levels at kinetochores

Robust SAC activity is essential for healthy and cancer cells alike; however, cancer transformation often alters SAC signaling (Kops et al., 2004). SAC amplification is more common in cancer, but in rare cases, tumor cells exhibit weakened checkpoint activity, resulting in aneuploidy (Saeki et al., 2002; Yuan et al., 2006; Choi et al., 2013). To test whether expression of E6 or E7 resulted in defective SAC signaling, we treated cells with 800 nM nocodazole for 16 h to depolymerize microtubules and activate the checkpoint. Under these conditions, 60–70% of RPE1, RPE17, and RPE167 cells were arrested in mitosis, whereas only 40% of RPE16 cells remained in mitosis (Figure 3A). This trend was also observed in immortalized lung fibroblasts expressing HPV16 proteins (Supplemental Figure 1D). Because a small population of RPE16 cells was observed to spend 100–200 min in mitosis, these data suggested that cells could generate a SAC response but could not sustain a mitotic arrest for prolonged periods; alternatively, RPE16 cells may enter mitosis less

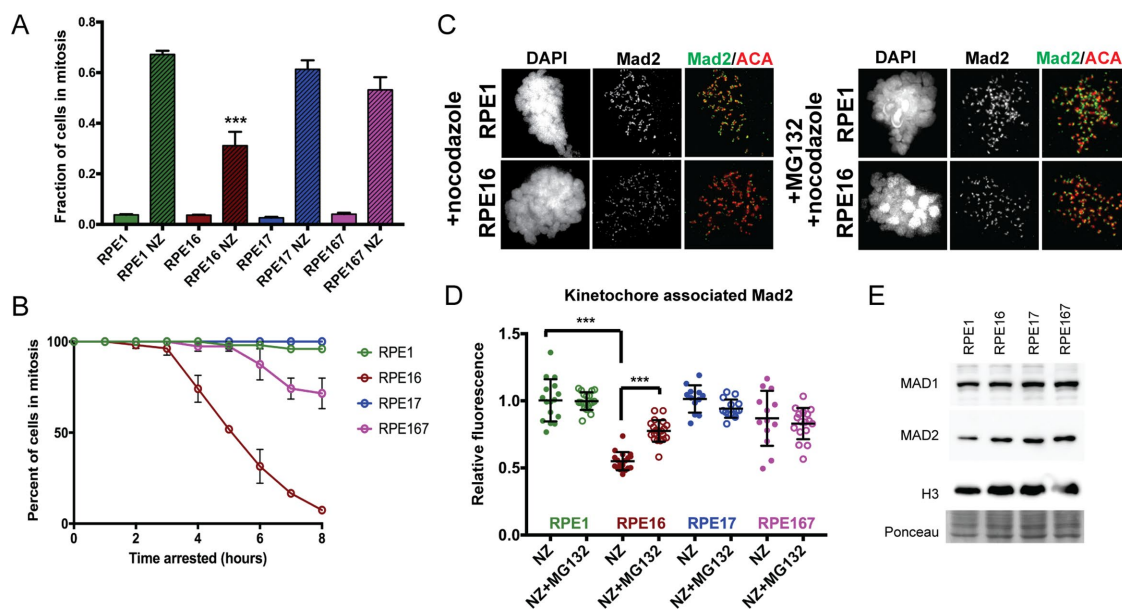


**FIGURE 3:** HPV E6-transformed cells exhibit defective SAC signaling and recruit less Mad2 to kinetochores. (A) Mitotic index of control cells (solid) and cells arrested in 800 nM nocodazole for 16 h (striped) and then fixed. More than 200 cells analyzed among replicates. (B) Quantification of time-lapse analysis of duration of mitotic arrest in nocodazole-treated cells. Only cells entering mitosis and exiting or arresting >8 h during the filming period were analyzed. Mean values and SD from three experiments with >60 cells analyzed. (C) Representative images and (D) quantification of kinetochores-associated Mad2 in each cell line arrested with nocodazole (solid circles) and in the presence of proteasome inhibitor MG132 (open circles). (E) Total cellular levels of MAD2 and MAD1 determined by immunoblot with histone H3 loading control. All error bars are SD of mean kinetochores intensity per cell from three experiments. Two-sided Student's t test, \*\*\* $p < 0.001$ .

frequently. We observed the former via live-cell imaging, in which most RPE16 cells maintained a mitotic arrest for only ~3 h and nearly all cells exited mitosis within 8 h (Figure 3B). RPE167 cells began exiting mitosis at ~5 h in nocodazole, whereas RPE1 and RPE17 cells arrested for >8 h (Figure 3B).

Mad2 kinetochore levels correlate with a cell's ability to sustain a mitotic arrest in response to spindle poisons such as nocodazole and Taxol. Thus we immunostained E6- and E7-transformed cells using Mad2 antibodies (Collin *et al.*, 2013). Cells were treated with 10  $\mu$ M nocodazole for 30 min after a double-thymidine block to generate completely unattached kinetochores and maximize Mad2 localization. Under these conditions, Mad2 kinetochore levels in RPE17 cells were similar to those in RPE1 cells, whereas levels were reduced by ~50% in RPE16 cells (Figure 3, C and D). The simultaneous expression of E6 and E7 resulted in an intermediate phenotype in which Mad2 levels were reduced by ~15% from RPE1 levels. These results indicate that failure to sustain SAC signaling is due in part to loss of kinetochore-associated Mad2.

### Kinetochore-associated Mad2 levels increase after inhibition of the 26S proteasome

HPV16 E6 binds to the ubiquitin ligase E6AP/UBE3A, causing polyubiquitination and subsequent degradation of noncanonical UBE3A targets, including p53 (Scheffner *et al.*, 1993; Takizawa *et al.*, 2006). To determine whether changes to the ubiquitin-mediated degradation machinery are responsible for loss of Mad2 at RPE16 kinetochores, we treated cells that had been synchronized through a double-thymidine block with a proteasome inhibitor, MG132. Proteasome inhibition did not change Mad2 kinetochore levels in RPE1, RPE17, or RPE167 cells, but kinetochore levels increased in RPE16 cells from 50 to 80% of RPE1 cells. Thus changes to the proteasomal degradation pathway in E6-expressing cells decrease Mad2 kinetochore levels and likely contribute to the inability of these cells to sustain a prolonged SAC arrest. It is unlikely that this is due to increased turnover of Mad2 itself in E6-expressing cells because, by immunoblot, total Mad2 levels are elevated compared with RPE1 (Figure 3E). The protein levels of Mad2's binding partner at kinetochores, Mad1, are also unchanged in E6-expressing cells (Figure 3E).

### Cells expressing E6 are prone to cohesin fatigue, likely due to elevated WAPL levels

The SAC defect in E6-expressing cells was obvious only because of the pole-associated chromosomes, which required sustained SAC activity. Pole-associated chromosomes are commonly observed when kinetochore-microtubule attachments are hyperstabilized (DeLuca *et al.*, 2011; Caldas *et al.*, 2013; Tauchman *et al.*, 2015). To determine whether expression of E6 results in hyperstable attachments, we measured the distance between sister kinetochores of bioriented, aligned chromosomes in our cell lines. Interkinetochore distances of bioriented sister kinetochore pairs in control RPE1 cells were on average ~1.22  $\mu$ m, and similar distances were measured on bioriented sister kinetochore pairs in RPE17 cells (~1.20  $\mu$ m). Interkinetochore distances in RPE167 cells were shorter on average (~1.07  $\mu$ m; Figure 3A). Of interest, interkinetochore distances of bioriented sister kinetochore pairs in RPE16 cells exhibited a bimodal distribution (Figure 3B). Most sister kinetochore pairs in RPE16 cells exhibited interkinetochore distances similar to those measured in RPE167 cells (~1.07  $\mu$ m), but a small population of sister kinetochores in RPE16 cells had significantly longer interkinetochore distances (~1.63  $\mu$ m), consistent with either kinetochore-microtubule attachment hyperstability or premature chromatid separation. This second population was entirely composed of RPE16 cells, with a few pole-associated chromosomes and

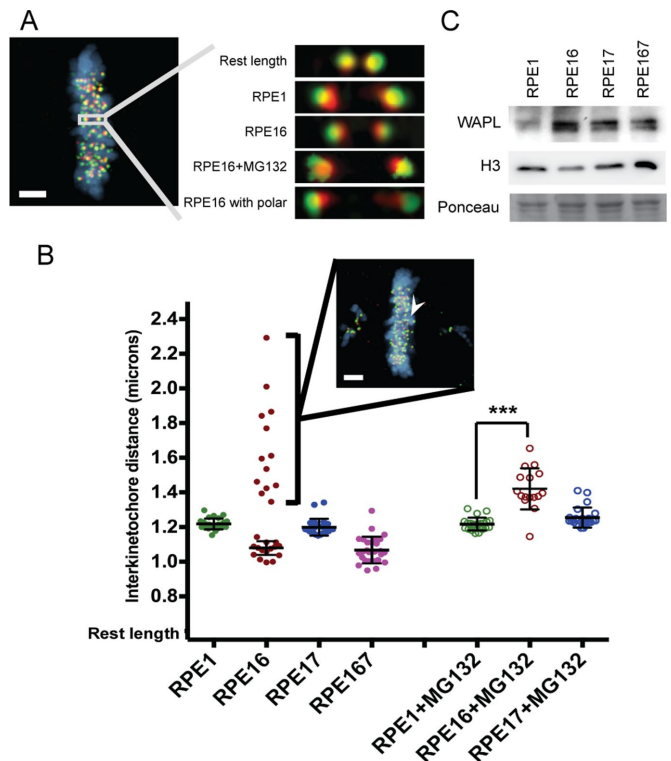


**FIGURE 4:** HPV E6-expressing cells cannot maintain robust sister chromatid cohesion during prolonged mitosis. (A) Representative image of metaphase cell used to measure average interkinetochore distances and representative images of sister kinetochores for cell lines of interest. Interkinetochore distances measured between Hec1 foci (green) separated by ACA (red) staining. (B) Average interkinetochore distance between bioriented sister kinetochores per cell for untreated RPE cells (solid circles) and MG132-treated cells (open circles). RPE16 cells that undergo delayed mitoses due to polar chromosomes (inset) or MG132 treatment (open circles) experience premature sister chromatid separation and abnormally long IKDs on bioriented sister kinetochores. (C) Western blot of cellular WAPL levels in E6/E7-expressing cells. Scale bars, 2  $\mu$ m; error bars are SD of mean interkinetochore distance per cell from three experiments. Two-sided Student's *t* test, \*\*\**p* < 0.001.

an aligned metaphase plate from which interkinetochore distances were measured (Figure 4B). As mentioned, cells with this phenotype spent an average of 80 min in mitosis, which suggested that the increased interkinetochore distances might be due to cohesin fatigue and premature sister chromatid separation after a prolonged arrest rather than attachment hyperstability (Daum *et al.*, 2011).

To understand whether this fatigue was unique to RPE16 cells, we again treated RPE1, RPE16, and RPE17 cells with MG132 to inhibit the proteasome. Previous studies demonstrated that such treatment prevents anaphase onset and prolongs the time cells spend in metaphase, eventually resulting in cohesin fatigue (Daum *et al.*, 2011). We treated cells with 10  $\mu$ M MG132 for 80 min (the average mitotic duration of RPE16 cells with polar chromosomes) and measured interkinetochore distances (Figure 4B). The average interkinetochore distance of aligned sister kinetochore pairs in RPE1 and RPE17 cells was largely unchanged from that in untreated cells (~1.22 and ~1.24  $\mu$ m, respectively). In contrast, the average interkinetochore distance of aligned sister kinetochore pairs in RPE16 cells was significantly longer (~1.42  $\mu$ m), supporting the idea that E6 expression results in perturbed cohesin function.

Consistent with this finding and previous studies, we found that E6-expressing and, to a lesser extent, E7-expressing cells increase protein levels of a cohesin antagonist, WAPL (Figure 4C). Although the average interkinetochore distance did not significantly increase in E7 cells after 80 min in MG132, a small number of cells exhibited increased interkinetochore distances, suggesting that E7 cells may undergo fatigue sooner than RPE1 cells as well (Figure 4B).

### Model for E6 and E7 contributions to chromosome segregation errors

We determined that HPV E6 increases the incidence of mitotic slippage and premature sister chromatid separation; however, these defects result in aneuploidy only after mitotic delays. We found that E6 expression induced mitotic delays by compromising biorientation of one to four chromosomes that instead remained associated with spindle poles. Thus, in cycling cells, these combined perturbations increase genetic instability.

We found that pole-associated chromosomes are likely not the result of hyperstable kinetochore–microtubule attachments, despite such attachments being linked to aneuploidy (Cimini, 2008). Although we did not determine the molecular mechanism responsible for this phenotype, it is possible that expression of E6 results in the misregulation of factors that contribute to chromosome congression, such as CENP-E, EB1, CLIP170, or adenomatous polyposis coli (APC; Green *et al.*, 2005; Tanenbaum *et al.*, 2006; Wood *et al.*, 2010). APC is of particular interest because its depletion also results in loss of the protein Bub1, which functions to recruit Mad2 to kinetochores (Kaplan *et al.*, 2001; Dikovskaya *et al.*, 2007).

E6 expression weakens the ability of the SAC to sustain a robust arrest in response to misaligned chromosomes, in part due to decreased Mad2 levels at kinetochores. This is consistent with previous findings in RPE1 cells showing that Mad2 levels directly correlate with length of SAC arrest (Collin *et al.*, 2013). However, E6 expression appears to increase total Mad2 protein levels, suggesting that this is instead a result of defective kinetochore recruitment. We also found that inhibition of the 26S proteasome partially rescued Mad2 kinetochore levels, indicating that a proteolytic event decreases Mad2 kinetochore recruitment. This proteolytic event does not appear to target Mad2 or its binding partner Mad1, as their cellular levels do not change when HPV proteins are expressed (Figure 3E). Checkpoint activity at kinetochores is regulated by many proteins and enzymatic reactions, and thus will require further study.

Expression of E6 also induced mild cohesion defects resulting in premature sister chromatid separation (observed by interkinetochore distances) during mitotic delays. Premature separation of sister kinetochores causes them to form merotelic attachments contributing to aneuploidy (Daum *et al.*, 2011). This defect arises in part because of increased WAPL expression.

Chromosome segregation defects in RPE17 cells result from better understood phenomena. The most commonly observed error was lagging chromosomes at anaphase. It is possible that this error arises from cohesin fatigue. WAPL levels are increased in RPE17 cells, and a small number of cells demonstrated premature separation after an 80-min arrest. Moreover, E7's canonical activity of silencing pRB may also contribute to cohesion defects, as previously reported (Manning *et al.*, 2010). In unperturbed RPE17 cells, however, we rarely observed abnormally long interkinetochore distances or prolonged mitotic delays. Thus we suggest that defects in microtubule depolymerases, which have been well studied in multiple cancers, drive most chromosome segregation defects observed in E7 cells (Bakhoun *et al.*, 2009b).

When expressing E6 and E7 together, it appears that phenotypes associated with cell proliferation are additive (doubling time, anchorage-independent growth), whereas in mitotic assays, E6 dominates the RPE167 phenotypes. Of interest, RPE167 followed the same trends as RPE16 cells, but less dramatically. This is likely a result of HPV genomic structure. Both E6 and E7 are dicistronically transcribed from the internal p97 promoter, and translation of E7 is primarily dependent on precise splicing of the pre-mRNA (Halbert *et al.*, 1991; Zheng *et al.*, 2004). Owing to this splicing activity, RPE167 cells likely have lower soluble levels of E6 than those expressing E6 alone, despite being driven from the same promoter. We were unable to measure protein levels due to antibody detection capabilities via Western blotting.

It is well established that E6 and E7 inhibit tumor suppressor pathways, allowing aneuploid cells to persist rather than trigger senescence. We identified multiple ways in which these proteins contribute more directly to aneuploidy. E6 is of particular interest because it induced chromosome segregation errors not through a single defective pathway but instead by weakening multiple complementary pathways. In this case, chromosome congression defects delay mitosis, allowing aneuploidy to arise from cohesin fatigue and/or mitotic slippage. Although such subtle mitotic defects are more difficult to observe experimentally, they may be a key to understanding aneuploidy within cancer and its contributions to tumor evolution and heterogeneity.

Although failures in biorientation and mitotic slippage have been observed after experimental manipulations such as RNA interference, to our knowledge, they have not been documented as a result of cancer transformation. Decreased SAC activity has been suggested in some cancers due to their RNA transcription profiles; however it has not been demonstrated that this directly contributes to aneuploidy (Saeki *et al.*, 2002). A key step in understanding the source of genetic instability will be to validate these findings in patient isolates for HPV-positive solid tumors.

## MATERIALS AND METHODS

### Cell culture and immunostaining

RPE1 (American Type Culture Collection) and derivative cell lines were cultured in DMEM/F-12 (Life Technologies) and supplemented with 1× penicillin/streptomycin and 10% fetal bovine serum (FBS) at 37°C in 5% CO<sub>2</sub>. For synchronization, cells were double-thymidine blocked in the following manner: cells were treated with 2.5 mM thymidine for 16 h, followed by 8 h in regular medium, then 2.5 mM thymidine again for 16 h. After the second 16-h block, cells were washed out into regular medium for 10 h. In Mad2 quantification experiments, cells were treated with 10 μM nocodazole for 30 min after the 10 h. For Mad2 rescue experiments, cells were treated with 10 μM MG132 for 2 h at 8 h after release from the second thymidine block, followed by 30 min in 10 μM nocodazole before fixation. For Mad2 immunofluorescence, cells were first permeabilized with 1× PHEM (60 mM PIPES, 25 mM HEPES, 10 mM EGTA, 2 mM MgCl<sub>2</sub>)–0.5% Triton-X for 2 min and then fixed with 4% paraformaldehyde for 20 min.

### Western blotting

Cells were collected from the flasks with trypsin, pelleted in a table-top centrifuge, and raised in cold 1× phosphate-buffered saline (140 mM NaCl, 2.5 mM KCl, 1.6 mM KH<sub>2</sub>PO<sub>4</sub>, 15 mM Na<sub>2</sub>HPO<sub>4</sub>, pH 7.0), 2 mM dithiothreitol, and protease inhibitor cocktail (Thermo). Cells were sonicated on ice (Ultra Sonic Device), and lysates were clarified by centrifugation. Protein samples (40 μg) were run on 12% SDS–polyacrylamide gels and transferred

to polyvinylidene difluoride membrane (Millipore). Blots were probed with the following antibodies: rabbit anti-Mad2 (Ted Salmon), 1:500; rabbit anti-Mad1 (GTX109519; GeneTex), 1:500; rabbit anti-WAPL (gift from Hongtao Yu), 1:500; and rabbit anti-histone H3 (ab1791; Abcam), 1:500. Primary antibodies were detected using horseradish peroxidase-conjugated anti-mouse secondary antibody at a dilution of 1:10,000 (A00160; Gene Script) and visualized via chemiluminescence on an ImageQuant LAS 500 imager.

### Viral transduction

MMLV-based retroviral particles were generated as previously described (Serrano *et al.*, 1997). Briefly, packaging cells were transfected with pCMV-TAT and pCSIG to VSV-G pseudotype viruses and one of the following: pLXSN-HPV16E6, pLXSN-HPV16E7, or pLXSN-HPV16E6 (gifts from Denise Galloway). FuGENE 6 (Promega) transfection reagent was used at a 3:1 volume-to-mass ratio. Growth medium was replaced 24 h after transfection. Viral particle-containing supernatant media were harvested 48 and 72 h after transfection.

To perform viral transductions, RPE1 cells were grown in viral particle-containing supernatant medium for 24 h. This was repeated with fresh viral containing-supernatant medium for an additional 24 h. At 48 h after initial infection, cells were exposed to medium containing a negative selective pressure. Selection and outgrowth lasted ~3 wk before a stable polyclonal population was established.

### Reverse transcription PCR

Cells were grown to 80% confluency in two T75 flasks. RNA was extracted using the Qiagen RNeasy Midi Kit. The Qiagen OneStep RT-PCR Kit was used to visualize transcript expression. Primers were designed to amplify either 234 base pairs of E6 (forward, 5'-GCAACAGTTACTGCGACGTG-3'; reverse, 5'-GGACACAGTGGCTTTT-GACAG-3') or 200 base pairs of E7 (forward, 5'-GACAGCTCAG-AGGAGGAGG-3'; reverse, 5'-TGAGAACAGATGGGGCACAC-3'). Samples were run on a 1.8% agarose gel for band visualization.

### Population doubling times

Each cell line was seeded at 50,000 cells in 12 wells of a 24-well plate. Three replicates of each cell line were counted using a hemocytometer 24, 48, and 72 h after initial seeding. These data were fitted to the exponential equation  $Y = P_0 e^{rt}$ , with  $r$  the growth rate and  $t$  the time in hours.

### Soft agar growth assay

Culture dishes were coated with 1% agarose. Then 150,000 cells were mixed into a 0.6% agar to form a second layer. Agar was hydrated with DMEM/F-12 to cover the agarose. Cells were incubated for 6 d, when spheroid colonies were observed. An Olympus CK2 inverted compound microscope with a 10x/0.25 numerical aperture (NA) 160/0.17 Olympus objective was used to quantitate the number of colonies formed per field. A total of 20 frames were counted, and the average number of spheres per field was recorded.

### Antibodies

Cells were stained with the following primary antibodies at the given concentrations: rabbit anti-Mad2, 1:200 (a generous gift from Ted Salmon); human anti-ACA, 1:300 (15-235; Antibodies Incorporated); mouse anti-Hec1 [9G3], 1:2000 (GTX70268; GeneTex); mouse anti- $\alpha$ -tubulin [DM1a], 1:300 (T9026; Sigma-Aldrich).

### Chromosome spreads

Cells were arrested in metaphase by treating with Colcemid for 2 h at a final concentration of 100 ng/ $\mu$ l. Cells were harvested and

resuspended in 75 mM KCl for 40 min and then fixed with a 3:1 methanol:acetic acid solution. Cells were dropped onto coverslips and mounted with Prolong Gold antifade reagent containing 4',6-diamidino-2-phenylindole (P36931; ThermoFisher).

### Image acquisition and analysis

Images were acquired on a DeltaVision Personal DV (Applied Precision) imaging system equipped with a CoolSNAP HQ2 (Photometrics/Roper Scientific) camera with a 60x/1.42 NA PlanApochromat objective and SoftWoRx acquisition software (Applied Precision). Interkinetochore distances were measured in SoftWoRx as the distance from Hec1 centroid to Hec1 centroid, measuring only pairs that stained for both Hec1 and ACA within a single plane. Kinetochores intensities were also quantified using SoftWoRx, by which the integrated fluorescence intensity minus the calculated background was determined for each kinetochore on maximum projected images. Values from HPV-expressing cells were normalized to the average value obtained from RPE1 cells (Hoffman *et al.*, 2001).

### Live-cell microscopy

Transformed cells expressing GFP-H2B were seeded at 500,000 cells and imaged the next day for 16 h with or without immediate addition of 800 nM nocodazole. Cells were imaged in a 37°C environmental chamber (Pathology Devices) in Leibovitz's L-15 medium (Life Technologies) supplemented with 10% FBS, 7 mM 4-(2-hydroxyethyl)-1-piperazineethanesulfonic acid, and 4.5 g/l D-glucose (pH 7.0). Images were taken in three different z-stacks every 5 min at an exposure of 300 ms for a total of 16 h. Images were acquired on a Nikon Eclipse Ti Microscope (Nikon) equipped with an Andor Clara camera (Andor) and a 40x/0.75 NA Plan Fluorite DIC lens (Nikon).

### ACKNOWLEDGMENTS

We thank Denise Galloway (Fred Hutchinson Cancer Research Center) for kindly providing pLXN HPV16 vectors and also Hongtao Yu (UT Southwestern Medical Center) and Ted Salmon (University of North Carolina) for antibodies. We acknowledge funding from National Institutes of Health Grant R01GM088371 and a grant from the Phi Beta Psi National Sorority.

### REFERENCES

- Bakhom SF, Genovese G, Compton DA (2009a). Deviant kinetochore microtubule dynamics underlie chromosomal instability. *Curr Biol* 19, 1937–1942.
- Bakhom SF, Thompson SL, Manning AL, Compton DA (2009b). Genome stability is ensured by temporal control of kinetochore-microtubule dynamics. *Nat Cell Biol* 11, 27–35.
- Caldas GV, DeLuca KF, DeLuca JG (2013). KNL1 facilitates phosphorylation of outer kinetochore proteins by promoting Aurora B kinase activity. *J Cell Biol* 203, 957–969.
- Choi J-W, Kim Y, Lee J-H, Kim Y-S (2013). High expression of spindle assembly checkpoint proteins CDC20 and MAD2 is associated with poor prognosis in urothelial bladder cancer. *Virchows Arch* 463, 681–687.
- Cimini D (2008). Merotelic kinetochore orientation, aneuploidy, and cancer. *Biochim Biophys Acta* 1786, 32–40.
- Cimini D, Howell B, Maddox P, Khodjakov A, Degross F, Salmon ED (2001). Merotelic kinetochore orientation is a major mechanism of aneuploidy in mitotic mammalian tissue cells. *J Cell Biol* 153, 517–527.
- Collin P, Nashchekina O, Walker R, Pines J (2013). The spindle assembly checkpoint works like a rheostat rather than a toggle switch. *Nat Cell Biol* 15, 1–11.
- Daum JR, Potapova TA, Sivakumar S, Daniel JJ, Flynn JN, Rankin S, Gorbsky GJ (2011). Cohesion fatigue induces chromatid separation in cells delayed at metaphase. *Curr Biol* 21, 1018–1024.
- DeLuca KF, Lens SMA, DeLuca JG (2011). Temporal changes in Hec1 phosphorylation control kinetochore-microtubule attachment stability during mitosis. *J Cell Sci* 124, 622–634.

- Dikovskaya D, Schiffmann D, Newton IP, Oakley A, Kroboth K, Sansom O, Jamieson TJ, Meniel V, Clarke A, Näthke IS (2007). Loss of APC induces polyploidy as a result of a combination of defects in mitosis and apoptosis. *J Cell Biol* 176, 183–195.
- Duensing S, Münger K (2002). The human papillomavirus Type 16 E6 and E7 oncoproteins independently induce numerical and structural chromosome instability. *Cancer Res* 62, 7075–7082.
- Gordon DJ, Resio B, Pellman D (2012). Causes and consequences of aneuploidy in cancer. *Nat Rev Genet* 13, 189–203.
- Green RA, Wollman R, Kaplan KB (2005). APC and EB1 function together in mitosis to regulate spindle dynamics and chromosome alignment. *Mol Biol Cell* 16, 4609–4622.
- Halbert CL, Demers GW, Galloway DA (1991). The E7 gene of human papillomavirus type 16 is sufficient for immortalization of human epithelial cells. *J Virol* 65, 473–478.
- Hoffman DB, Pearson CG, Yen TJ, Howell BJ, Salmon ED (2001). Microtubule-dependent changes in assembly of microtubule motor proteins and mitotic spindle checkpoint proteins at Ptk1 kinetochores. *Mol Biol Cell* 12, 1995–2009.
- Kaplan KB, Burds AA, Swedlow JR, Bekir SS, Sorger PK, Näthke IS (2001). A role for the adenomatous polyposis coli protein in chromosome segregation. *Nat Cell Biol* 3, 429–432.
- Knowlton AL, Lan W, Stukenberg PT (2006). Aurora B is enriched at merotelic attachment sites, where it regulates MCAK. *Curr Biol* 16, 1705–1710.
- Kops GJPL, Foltz DR, Cleveland DW (2004). Lethality to human cancer cells through massive chromosome loss by inhibition of the mitotic checkpoint. *Proc Natl Acad Sci USA* 101, 8699–8704.
- Lara-Gonzalez P, Westhorpe FG, Taylor SS (2012). The spindle assembly checkpoint. *Curr Biol* 22, R966–R980.
- Liu X, Clements A, Zhao K, Marmorstein R (2006). Structure of the human papillomavirus E7 oncoprotein and its mechanism for inactivation of the retinoblastoma tumor suppressor. *J Biol Chem* 281, 578–586.
- Manning AL, Longworth MS, Dyson NJ (2010). Loss of pRB causes centromere dysfunction and chromosomal instability. *Genes Dev* 24, 1364–1376.
- Mori S, Chang JT, Andrechek ER, Matsumura N, Baba T, Yao G, Kim JW, Gatz M, Murphy S, Nevins JR (2009). Anchorage-independent cell growth signature identifies tumors with metastatic potential. *Oncogene* 28, 2796–2805.
- Musacchio A, Salmon ED (2007). The spindle-assembly checkpoint in space and time. *Nat Rev Mol Cell Biol* 8, 379–393.
- Saeki A, Tamura S, Ito N, Kiso S, Matsuda Y, Yabuuchi I, Kawata S, Matsuzawa Y (2002). Frequent impairment of the spindle assembly checkpoint in hepatocellular carcinoma. *Cancer* 94, 2047–2054.
- Scheffner M, Huibregtse J, Vierstra R, Howley P (1993). The HPV-16 E6 and E6-AP complex functions as a ubiquitin-protein ligase in the ubiquitination of p53. *Cell* 75, 495–505.
- Serrano M, Lin AW, McCurrach ME, Beach D, Lowe SW (1997). Oncogenic ras provokes premature cell senescence associated with accumulation of p53 and p16INK4a. *Cell* 88, 593–602.
- Shin SI, Freedman VH, Risser R, Pollack R (1975). Tumorigenicity of virus-transformed cells in nude mice is correlated specifically with anchorage independent growth in vitro. *Proc Natl Acad Sci USA* 72, 4435–4439.
- Takizawa S, Nagasaka K, Nakagawa S, Yano T, Nakagawa K, Yasugi T, Takeuchi T, Kanda T, Huibregtse JM, Akiyama T, Taketani Y (2006). Human scribble, a novel tumor suppressor identified as a target of high-risk HPV E6 for ubiquitin-mediated degradation, interacts with adenomatous polyposis coli. *Genes Cells* 11, 453–464.
- Tanenbaum ME, Galjart N, van Vugt MA, Medema RH (2006). CLIP-170 facilitates the formation of kinetochore-microtubule attachments. *EMBO J* 25, 45–57.
- Tauchman EC, Boehm FJ, DeLuca JG (2015). Stable kinetochore-microtubule attachment is sufficient to silence the spindle assembly checkpoint in human cells. *Nat Commun* 6, 8987.
- Thomas J, Laimins L (1998). Human papillomavirus oncoproteins E6 and E7 independently abrogate the mitotic spindle checkpoint. *J Virol* 72, 1131–1137.
- Thompson D, Belinsky G, Chang T (1997). The human papillomavirus 16 E6 oncoprotein decreases the vigilance of mitotic checkpoints. *Oncogene* 15, 3025–3035.
- Wood KW, Lad L, Luo L, Qian X, Knight SD, Nevins N, Brejc K, Sutton D, Gilmartin AG, Chua PR, et al. (2010). Antitumor activity of an allosteric inhibitor of centromere-associated protein-E. *Proc Natl Acad Sci USA* 107, 5839–5844.
- Yuan B, Xu Y, Woo J-H, Wang Y, Bae YK, Yoon D-S, Wersto RP, Tully E, Wilsbach K, Gabrielson E (2006). Increased expression of mitotic checkpoint genes in breast cancer cells with chromosomal instability. *Clin Cancer Res* 12, 405–410.
- Zheng ZM, Tao M, Yamanegi K, Bodaghi S, Xiao W (2004). Splicing of a cap-proximal human papillomavirus 16 E6E7 intron promotes E7 expression, but can be restrained by distance of the intron from its RNA 5' cap. *J Mol Biol* 337, 1091–1108.